Soft Matter

PAPER

View Article Online
View Journal | View Issue

Cite this: *Soft Matter*, 2014, **10**, 2365

Micro-topography influences blood platelet spreading†

Rabea Sandmann,[a] Sarah Schwarz G. Henriques,[a] Florian Rehfeldt[b] and Sarah Köster*[a]

Injuries in blood vessels are accompanied by disrupted endothelial cell layers. Missing or destroyed endothelial cells lead to rough, structured surfaces on the micrometer scale. The first cells to arrive at the site of injury and to cover the wound are platelets, which subsequently drive blood clot formation. Therefore, investigating the interactions of platelets with structured surfaces is essential for the understanding of blood clotting. Here, we study the effects of underlying topography on platelet spreading using microstructured model substrates with varying area fractions of protein coating. We thereby distinguish the effects of (physical) topography and of (biochemical) protein availability. By analyzing the cell area and morphology, we find that the extent of protrusion formation – but not the total spread area – is determined by the area fractions of coating. The extent of filopodia formation is influenced by the availability of binding sites and the reaction of cells to the substrate's topography. The cells react to the structured substrate by avoiding topographic holes at the cell periphery and thus adapting their outer shape. This finding leads us to the conclusion that both chemically blocked and fibrinogen-coated holes represent "energetic obstacles" to the cells. Thus, the shape of the cell is governed by the interplay between spreading to an optimized area and adaption to the substrate topography.

Received 13th October 2013
Accepted 23rd October 2013

DOI: 10.1039/c3sm52636d

www.rsc.org/softmatter

1. Introduction

Blood clot formation is life-saving in mammals but involves serious health risks when occurring under pathological conditions. Main players in blood clotting are blood platelets (thrombocytes), which despite their tiny size of 2–5 μm in diameter when quiescent,[1] exert great forces[2] that help to contract the blood clot. The great biomedical importance of this specialized cell type has led to detailed studies of platelet structure and function early on, tremendously furthering our understanding of the field.[3–5] As it is common practice in cell biology, almost all past studies have been performed using rigid, smooth substrates, such as glass slides or cell culture dishes. However, this is not what platelets encounter *in vivo*. Wounds arise from disrupted or destroyed endothelial cell layers in the lining of blood vessels and therefore constitute a "microstructured" surface. Extending this idea further, the proteins that lie underneath the endothelial cell layer and get exposed following an injury represent a "nanostructure". The first layer of platelets therefore encounters both nanostructures and microstructures. The situation is quite similar for the subsequent layers which activate on top of and attach to the existing clot. The result of this clotting process is schematically sketched in Fig. 1a.

Taking into account the *in vivo* environment of platelets, it is therefore clear that platelets encounter topographically and biochemically structured substrates while closing a wound. With the advent and rapid development of inexpensive and simple-to-use microstructuring and micropatterning techniques such as microcontact printing (MCP)[6,7] and soft lithography[8,9] it has generally become feasible to examine the effect of such substrates on various cell types. Numerous interesting findings have greatly helped to understand cell behavior in close-to-physiological environments. Several studies show that cells in principle sense nano- and microstructures[10–13] and might even be able to detect the radius of curvature of micro-holes in a substrate and thereby the size of the holes.[14] The mechanisms behind the interactions of cells and topographically structured substrates are not completely understood and are probably very complex. It has, for example, been suggested, that variations in reaction to topographies in different cell types can be attributed to different amounts of actin monomers in the cells.[15] The review by Bettinger *et al.*[11] sums up several theories on how cells can sense topography and react to it. Mostly, filopodia are believed to be one of the main players in topography sensing: they are involved, *e.g.*, in alignment of cells on ridges or grooves since filopod formation perpendicular to these features

[a]*University of Göttingen, Institute for X-Ray Physics, Friedrich-Hund-Platz 1, 37077 Göttingen, Germany. E-mail: sarah.koester@phys.uni-goettingen.de; Fax: +49-55139-9430; Tel: +49-55139-9429*

[b]*University of Göttingen, Third Institute of Physics – Biophysics, Friedrich-Hund-Platz 1, 37077 Göttingen, Germany*

† Electronic supplementary information (ESI) available. See DOI: 10.1039/c3sm52636d

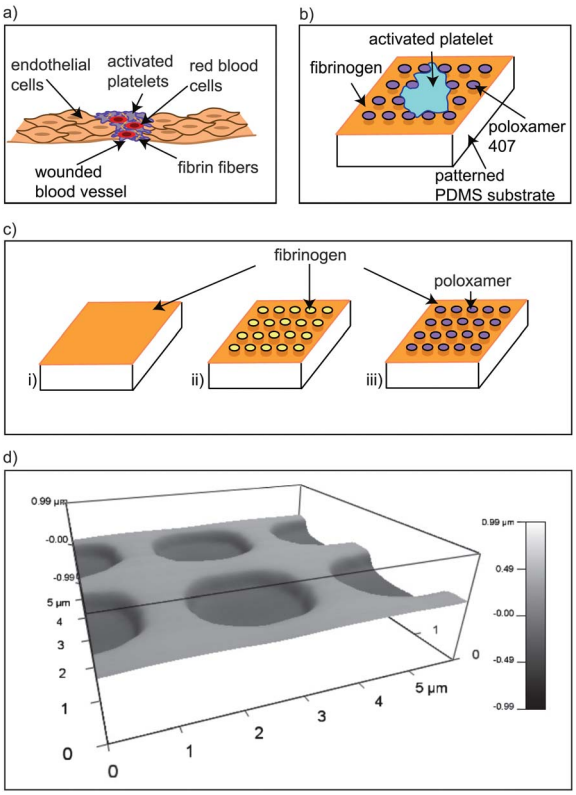

Fig. 1 (a) Schematic representation of early hemostasis in a wounded blood vessel. (b) Model substrates to mimic effects of topography and biochemical clues in early stages of hemostasis. (c) Schematic representation of the three different substrate types. The flat substrates (i) are completely coated with fibrinogen, whereas the structured substrates are either (ii) completely coated with fibrinogen or (iii) only the elevated parts are coated while the holes are blocked with poloxamer 407. (d) AFM image of the PDMS substrate to which a plane fit in the *x*/*y* direction (Igor Pro 6.22A, MFP-3D software) was applied. The picture shows that the hole walls are quite steep.

causes intracellular stresses and is therefore not favored. Furthermore, alignment of cells and morphological changes due to cell–substrate interactions are believed to arise from modification of focal adhesion geometry or localization due to geometrical constraints. Lim *et al.*[16] included both chemical patterning and topography in their review.

Owing to their great biomedical importance, platelet studies have traditionally been performed in the medical and clinical fields.[17–19] Above, we have focused on the physiological context of platelets and their interaction with proteins and other cells. However, platelets are not only first to arrive at a newly wounded tissue but also the first cells to cover implants when the material is placed in the body. It has been shown that platelet activity is influenced by microstructured surfaces of (titanium) implants. Interestingly, the influence applies not only to the first layer directly on the substrate but also to more remote layers.[20] By testing the effects of platelets more systematically on defined and reproducible structures, Zhou *et al.*[21] attributed the different degrees of platelet spreading to differences in substrate hydrophobicity, whereas Chen *et al.*[22] showed that substrate topography influences adsorption of proteins which platelets then in turn encounter. The fact that protein distribution itself can influence platelet behavior without any underlying topography was also shown by Kita *et al.*[23] By investigating the behavior of single platelets on substrates stamped with proteins they showed that platelets use their filopodia to sense the environment. Furthermore, they found that on chemically structured substrates with no underlying topography platelets can span uncoated regions as broad as 5 µm.

Despite the importance for biology and medicine, studies including both topographic structures and chemical patterns (as depicted in Fig. 1b) at the single platelet level, are, to the best of our knowledge, still lacking. We show that platelets react to both topography and protein coating of the substrate, albeit in different ways. To investigate the response of single platelets to topographically structured substrates, we used a structured PDMS surface as a simple model system, in which fibrinogen acts as a mediator to allow platelets to adhere to the surface. The geometry of the structures and the coating with fibrinogen are chosen to mimic interactions of platelets with the first layer of platelets on implants or wounded tissue. We place individual platelets on (i) flat, completely coated, (ii) topographic, completely coated and (iii) topographic, selectively coated substrates as shown in Fig. 1c, and analyze their size upon spreading, as well as their membrane outline. In a direct comparison between the substrate types we find that cells seek to achieve an optimized spread area independent of the substrate type but they adapt their cell outline, lamellipodia formation and local curvature to the topography of the substrate as well as to the availability of potential binding sites defined by the proteins on the surface.

2. Materials and methods

2.1. Substrate preparation

Micropatterns are designed in AutoCAD and transferred to a silicon wafer (Silchem, Freiberg, Germany) *via* conventional photolithography. We use a 1 : 1 mixture of SU-8 2001/SU-8 2000 thinner (both MicroChem, Newton, MA, USA) yielding a structure height of 505 (±25) nm. We thus capture the order of magnitude of the height of cells and thereby the topographical features in a wound. Platelets adhere to the disrupted endothelial cell layer and also in subsequent layers to other platelets. Platelets can be as thin as a few tens of nm (ref. 24) at the periphery when fully spread, while other cells are usually thicker (up to several µm). The structured substrates consist of an array of 2.1 (±0.1) µm diameter holes arranged in a square grid with 0.9 (±0.1) µm interspaces. Data for holes with a diameter of 2.8 (±0.1) µm and 1.1 (±0.1) µm interspaces are shown in the ESI.† The wafer is coated with (heptafluoropropyl)-trimethylsilane (97%, Sigma-Aldrich, München, Germany) to ensure easy detachment of PDMS (polydimethylsiloxane). PDMS with the cross-linker (10 : 1 weight mixture) (Sylgard 184, Dow Corning, Midland, MI, USA) is spincoated onto the wafer to yield a thin PDMS layer of 47 (±5) µm and it is baked for 1 hour at 80 °C on a hotplate. The cured PDMS is transferred, upside down, to a standard coverslip.

To distinguish between the effects of topographic and chemical (protein) patterns, we fabricate three different types of substrates. First, flat, non-structured substrates are completely coated with protein. Second, structured substrates are coated completely. Third, only the elevated parts of the structured substrate (*i.e.* the interspaces between the holes) are coated. The three substrate types are shown in Fig. 1c. To coat a substrate completely, it is activated by oxygen plasma treatment for 1.5 min. The plasma treatment renders the surface hydrophilic and negatively charged, ensuring that only weak interactions between the surface and the protein are present and the fibrinogen remains close to its native state.[25] A fluorescent fibrinogen solution (Alexa Fluor 488 conjugate, Life Technologies GmbH, Darmstadt, Germany, from human plasma, 0.05 mg mL^{-1}) is prepared and the solution is left on the substrate for one hour and subsequently removed, the substrate is washed three times with phosphate buffered saline (PBS) and let dry or kept immersed in PBS. This procedure ensures that the substrate is saturated with bound fibrinogen. For selectively coated substrates, microcontact printing as described by Bernard *et al.*[6] is employed. Briefly, the structured PDMS substrate is activated by oxygen plasma treatment for 1.5 min. A flat PDMS stamp (cured, 10 : 1 weight mixture) is soaked in the fibrinogen solution for 1 hour and then washed two times, each time for 5 seconds, in fresh MilliQ water and dried with N_2 is placed on top of the structured substrate for 15 minutes and weighed down with about 15 g. When comparing cells on flat stamped and immersed substrates we observe equivalent cell behavior, indicating a corresponding number of binding sites. The microcontact-printed substrate is then treated with poloxamer 407 (poly(ethylene glycol)-*block*-poly(propylene glycol)-*block*-poly(ethylene glycol), 0.2%, Sigma-Aldrich, München, Germany) for 2 hours to block unspecific binding sites.[26] The poloxamer solution is removed and the substrate is washed three times with PBS. Afterwards, both the completely and the selectively coated substrates are washed three times with Medium 199 (with Earle's Balanced Salt Solution, L-glutamin and 25 mM Hepes Lonza, BioWittaker, Basel, Switzerland). Micrographs showing the quality of coating are depicted in Fig. S1 in the ESI.† As can be seen in Fig. 4 the holes are not perfect squares but have rounded corners. Thus, the curvature is higher at the corners. We determine the mean local radius of curvature at the corners to be 2.0 ($\pm$0.1) μm^{-1}.

2.2. Platelet preparation

Platelets are purified from thrombocyte concentrates as described previously[2] with the centrifugation steps performed at 18–22 °C. The experiments are performed according to national and regional laws and with the consent of the Ethic Committee of the University of Göttingen and its ethical vote 11/11/09. In total, cells from twelve healthy donors were used. After purification, platelets are diluted to a concentration of 6×10^7 platelets per mL. 150 μL of the diluted cell suspension are placed on the substrates and platelets are allowed to settle on the surface for 15 minutes at room temperature. Next, 50 μL of thrombin solution (from human plasma, Sigma-Aldrich, München, Germany, 4 U mL^{-1}) are added to the solution to yield a final concentration of 1 U mL^{-1} and the samples are placed in an incubator at 37 °C and 5% CO_2-concentration for 60 minutes. Afterwards, 200 μL of 4% formaldehyde (FA, ~4 °C, diluted in PBS from 37% stabilized FA solution, Merck, Darmstadt, Germany) are added to the samples, which are then placed in the incubator for additional 20 minutes. The samples are subsequently washed three times with PBS. 200 μL of Alexa Fluor 594 phalloidin (Life Technologies) are added to the sample to yield a final concentration of 4.88 U mL^{-1} and left to react with the platelets for 30 minutes at room temperature. After washing the samples again three times with PBS, the substrates are mounted with Prolong Gold antifade reagent solution (Life Technologies). During storage, the platelets are likely to be already activated in solution and interactions between the cells, just as in the *in vivo* situation, are probable. However, we restrict data acquisition and analysis to single platelets on the substrate.

2.3. Data acquisition and analysis

For image acquisition an inverted motorized research microscope (IX81, Olympus, Hamburg, Germany) equipped with a 100× oil-immersion phase contrast objective and the image acquisition software xcellence rt is used. At each investigated position on the sample both a phase contrast image and two fluorescence images, each of them with an acquisition time of 60 ms, are recorded to visualize the underlying substrate structure as well as the actin structure (Alexa Fluor 594) of the platelets and the fibrinogen coating (Alexa Fluor 488) of the substrate. Data preprocessing requires a selection of platelets that are completely spread and isolated from (not covered by or lying on top of) other platelets or irregular fibrinogen coating. Afterwards, the contours of the cells are detected in the fluorescence images by a program written in MATLAB (MATLAB R2009b, The MathWorks, Inc., Natrick, MA, USA) using the Canny edge detection algorithm with a low threshold of 0 and a high threshold of 0.05. The outlines as detected before are connected by hand and filled to create masks of the cells. In cases, where the Canny algorithm fails to detect certain parts of the cells (*e.g.* those that are too faint as compared to the rest of the cell) these parts are drawn manually based on the fluorescence image. The different steps of image processing are shown in Fig. S2 in the ESI.† Typical phase contrast images of the substrate structure and the detected cell contours from the corresponding fluorescence image are shown in Fig. 4. Here, the cell contours are redrawn by hand after automatic detection to improve visibility. The area and perimeter of the cell are determined in ImageJ[27] and an ellipse is calculated that has the identical area and major and minor axes of the cell as described by Zemel *et al.*[28] Membrane curvature is computed by a program written in MATLAB that fits a spline function to the cell's contour in inverted binarized images (see Fig. S2c†), and evaluates the curvature of the outline of the cell by the second derivative of the fitted spline.

2.4. Atomic force microscopy (AFM) measurements

The substrate for the atomic force microscopy (AFM) images was produced as described above, activated for 1.5 minutes by

oxygen plasma treatment and immersed in PBS for the measurement. Images of the substrate topography are recorded with an MFP-3D (Asylum Research, Santa Barbara, USA) AFM and an Olympus OMCL-AC-240-TS cantilever (Atomic Force F&E GmbH, Mannheim, Germany) in AC mode at a scan rate of 0.25 Hz with a resolution of 256 × 256 points for a total field of view of 9 × 9 μm^2.

3. Results and discussion

3.1. Cell area

Complete platelet spreading is observed on the fibrinogen coated PDMS substrates as has been reported before, for example, for fibrinogen coated polysterene dishes (see Savage *et al.*[29]). In contrast to spreading of simple liquids where the spread area is determined by the interfacial energies of the involved materials, we here deal with a complex, active, viscoelastic material. In our experimental scenario, two parameters could influence the spreading area: the area fraction of the coating *via* the availability of binding sites and the substrate topography. We analyze platelets on all substrates used and compare the spreading area, as shown in Fig. 2 for holes with a diameter of 2.1 μm. Corresponding data, also for the following analyses, for holes with a diameter of 2.8 μm are presented in the ESI.†

Notably, the cell size is conserved within the accuracy of the measurement errors and is approximately 30 μm^2 for all substrate types and hole dimensions. This is consistent with the result that Lehnert *et al.*[30] have described for fibroblasts and mouse melanoblasts, which shows that optimal spreading is achieved for protein surface coverages of more than 15% (percentage of covered area with respect to total area) of the total substrate area. It is likely that the spreading to an optimal area of about 30 μm^2 is related, *via* the volume of the cells, to an optimal height and distribution of the force-generating machinery in the cells.

3.2. Cell shape and morphology

Although the spreading area of the platelets is conserved regardless of the topography of the substrate and the area fraction of the coating, the cell morphology is considerably influenced. Platelets on flat substrates display a rather smooth outline with few protrusions as shown in Fig. 3a. By contrast, platelets on completely coated, structured substrates display some broad protrusions (Fig. 3b) and platelets on selectively coated, structured substrates show even more pronounced lamellipodia (Fig. 3c). To quantify this observation, we analyze the ratio of cell perimeter U_{cell} to the perimeter of a calculated ellipse $U_{ellipse}$ with equal area. The perimeter of the calculated ellipse is determined based on the semi-major axis a and semi-minor axis b:[31]

$$U_{ellipse} = \pi(a+b)\left(1+\frac{3\lambda^2}{10+\sqrt{4-3\lambda^2}}\right) \quad (1)$$

with

$$\lambda = (a-b)/(a+b).$$

The histograms displayed in Fig. 3d show that platelets on structured substrates show a larger relative perimeter than the platelets on flat substrates and that the effect is more pronounced when the substrate is selectively coated. The ratio

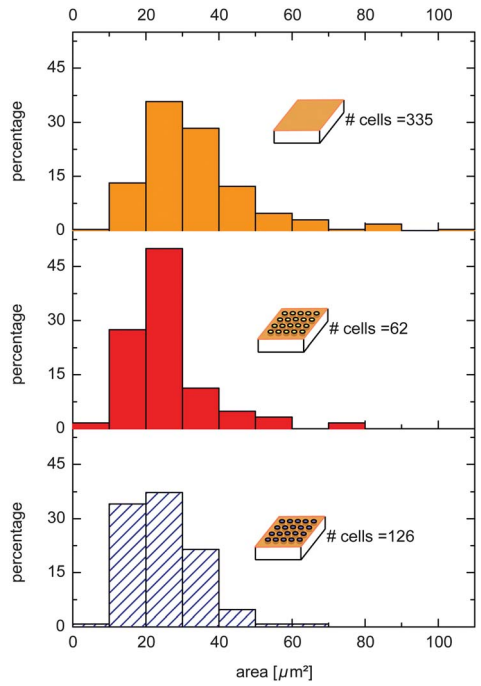

Fig. 2 Histograms showing the cell area of platelets on three different types of substrates: (top) on flat, completely fibrinogen-coated substrates; (center) on topographically structured, completely fibrinogen-coated substrates; (bottom) on topographically structured, selectively fibrinogen-coated substrates. The spreading area lies in the same range for all substrate types.

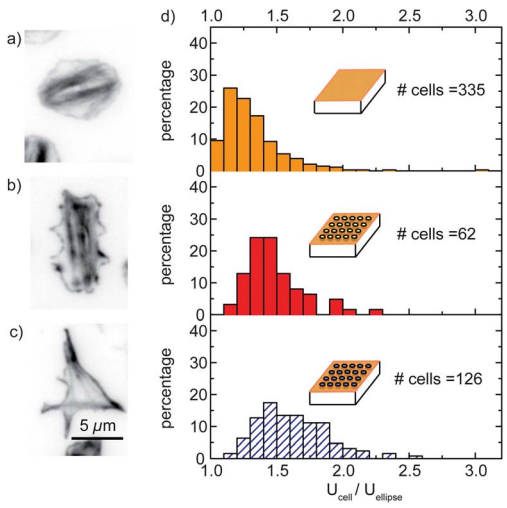

Fig. 3 (a–c) Typical cell morphologies in fluorescence images (stained for filamentous actin) on substrates with 2.1 μm wide holes. (d) Histograms showing the ratio of the cell perimeter U_{cell} to the perimeter of an ellipse $U_{ellipse}$ that has the same area as the cell for platelets on different substrates, for cells on substrates with 2.1 μm wide holes. The ratio increases from top to bottom.

of the cell perimeter U_{cell} to the perimeter of the calculated ellipse $U_{ellipse}$ accounts for cell–cell variations in the aspect ratio (semi-major axis divided by semi-minor axis). Higher values therefore clearly result from a roughened outline rather than from a more elliptical shape.

From the histograms and the images of the cells shown in Fig. 3 we conclude that platelets are in neither case perfect ellipses and that there is roughening of the cell outlines from flat over completely coated to selectively coated substrates. We explain this difference in cell morphology on the different substrates by the number and distribution of available binding sites. Platelets on flat, completely coated substrates adhere to the substrate with the desired spread area (see above) being the only condition to guide their shape. It is known that cells use protrusions like filopods to search for appropriate binding sites. In agreement with this concept we observe more protrusions on topographically structured substrates. If the substrates are completely coated with fibrinogen, binding sites are available but in a different geometric plane than the initial plane of cellular adhesion. The situation is even more striking for selectively coated substrates, where no binding sites are present inside the holes. These scenarios may explain the need for increased lamellipodia formation on topographically structured substrates.

3.3. Adaption to substrate topography

The availability of binding sites as explained above may account for the different cell morphologies on completely or selectively coated substrates, but fails to explain why cells on topographically structured, completely coated substrates display such a high number of lamellipodia: topography itself seems to play an important role.

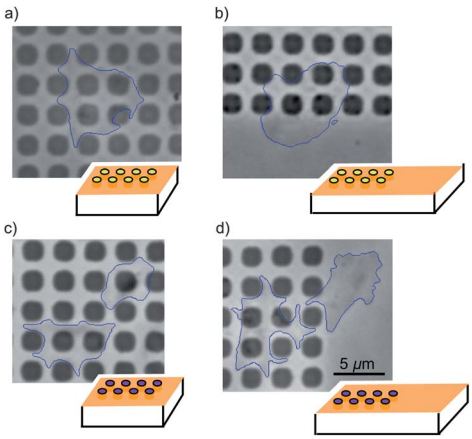

Fig. 4 Examples of phase contrast micrographs of cells on substrates with contours amplified in blue on substrates with 2.1 μm wide holes. (a) Platelets on completely coated, topographically structured substrates. (b) Platelets on completely coated substrates, partly lying on topographically structured parts and partly lying on flat parts. (c) Platelets on selectively coated, topographically structured substrates. (d) Platelets on selectively coated substrates, partly lying on topographically structured parts and partly lying on flat parts. Platelets adapt to the underlying substrate topography regardless of the area fraction of coating. Cells partially lying on flat and structured substrates are not included in the quantitative analysis.

As shown in Fig. 4, platelets adjust to the underlying topography by avoiding the holes at their periphery, whether the holes are coated with fibrinogen, as in Fig. 4a and b, or chemically blocked as in Fig. 4c and d. The direct transition from flat to structured substrates is shown in Fig. 4b and d. A clear difference can be observed between the behavior on flat substrates, where the membrane mainly follows a smooth line and on structured substrates, where platelets adapt their membrane to the underlying topography.

This effect can be observed for different hole dimensions on the substrates, as shown in Fig. 5 for hole sizes ranging from 2.8 μm to 1.0 μm. The larger the holes are, the more likely the extension of protrusions into fibrinogen-coated holes (in the case of completely coated substrates). For an example of a platelet that extends lamellipodia into the holes see the video M1 of a *z*-stack and Fig. S6 in the ESI.†

Membrane curvature is energy driven and thus, devoid of any additional boundary conditions, the membrane area at the periphery (or perimeter in a quasi-2D system as we investigate it here) is minimized leading to spherical (circular) shapes. The rather smooth cell contours we observed on flat substrates mirror exactly this energy minimization (under the influence of

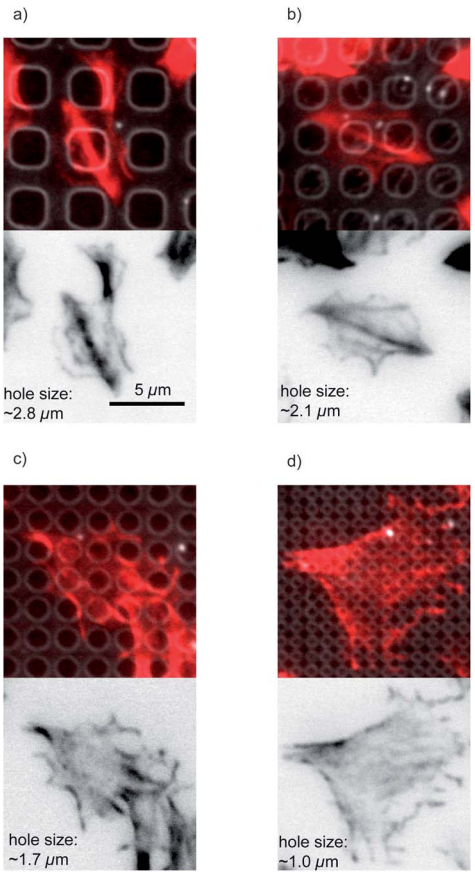

Fig. 5 Micrographs of cells on completely coated substrates with different hole sizes ranging from 2.8 μm to 1.0 μm in width. The upper micrographs show a combination of images from the stained actin of cells (red) and the fibrinogen coating (gray). The lower inverted ones show only the actin staining. The cells show adaption to the underlying substrate in all cases.

certain intra- or extracellular boundary conditions; contours are therefore not perfectly circular). This is also confirmed by the decay that we can observe in the histogram of curvature distribution for flat substrates (inset of Fig. 6a).

On structured substrates the cell outline follows the topography. The outline of the holes does not have a constant curvature, but is higher at the corners with $R^{-1} = 2\ \mu m^{-1}$ (marked cyan in the inset of Fig. 6b) and fairly small at the edges (marked orange in the inset of Fig. 6b), where it can be estimated as $R^{-1} \lesssim$ (hole radius)$^{-1}$. These two curvatures are reflected in the measured curvatures of the membrane. This becomes apparent, when analyzing the differences in membrane curvatures (Δ percentage) upon placing the cells on topographic structures, as shown in Fig. 6. For the completely coated substrates (Fig. 6a) we observe two peaks in the difference histogram, *i.e.* curvatures which are *more* pronounced on structured than on flat substrates. The smaller peak at around $R^{-1} = 2.0\ \mu m^{-1}$ corresponds to the corner radius, whereas the peak at around $R^{-1} = 1.0\ \mu m^{-1}$ corresponds to the hole radius. This second peak is due to the fact that for completely coated substrates the cells do find binding sites at the substrate walls and can therefore partly span over the holes. In agreement with this observation, for selectively coated substrates (Fig. 6b) the ratio of the heights of the peaks changes dramatically. In this case, the cells even more closely follow the contours of the holes. Compared to flat substrates we observe a decrease in the distribution for values smaller than about $R^{-1} = 0.6\ \mu m^{-1}$ for both structured substrates. For cells on substrates with 2.8 μm wide holes (see ESI†) the influence of the straight edges of the holes as compared to the rounded corners becomes stronger. On selectively coated substrates, where the cells closely follow the contours of the holes, this leads to an increase in the values for small curvatures as compared to flat substrates. In the difference diagram a peak for very small values emerges.

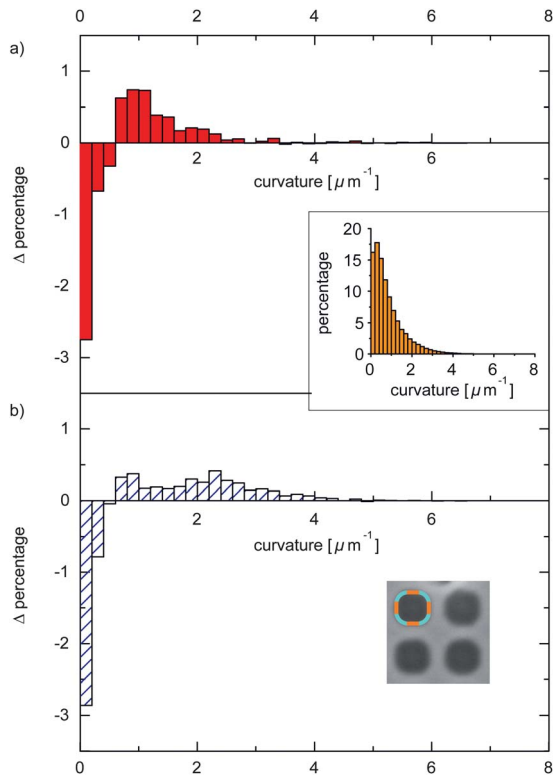

Fig. 6 Histograms showing the differences in average membrane curvature of platelets on different substrate types: (a) on completely coated, topographically structured substrates as compared to platelets on flat substrates; the difference value Δ percentage between both histograms is shown; the inset shows the corresponding histogram of platelets on flat substrates; (b) on selectively coated, topographically structured substrates as compared to platelets on flat substrates; the inset shows the different curvatures along the contour of the holes.

Taken together, we thus observed that platelets adapt their membrane curvature to the curvature of the holes in the underlying topography, at least at their periphery. This behavior can be understood by considering the options the cell has when encountering holes on the substrate. Since the cross-section of the holes is approximately rectangular with sharp edges, as it is typical for SU-8 lithography and can be seen in the AFM image of the structure in Fig. 1d, the curvature right at the edges of the holes is extremely high. For small holes, cells that seek to extend filopods inside the holes need to follow this high curvature with their membrane and cytosol. For larger holes, a (partial) detachment of the cell from the binding sites is imaginable.

In principle, cells are non-equilibrium systems which are able to recruit energy in the form of ATP to reach certain states. Our observation from this experimental setup is, however, that the cells avoid the holes by spreading around the structures. Thus, instead of paying the high energy costs to achieve high curvatures and thus be able to bend into the holes, the leading edges bend around the holes as seen in Fig. 4 and 5. The larger the holes are, the more likely it is that cells extend protrusions into the fibrinogen-coated holes (completely coated substrate). The larger diameter of holes provides the possibility to bend into the holes but with a larger bending radius. The confocal *z*-stack in the ESI† shows an example for such an event.

4. Conclusions

In conclusion, we have shown that the cells spread to an area of approximately 30 μm^2 regardless of the substrate topography or the area fraction of coating. Apparently, this optimal area is reached with minimized energy consumption for the respective situation. At their periphery, platelets avoid small holes as bending into the holes requires smaller radii of curvature than bending around the holes. This interplay between fixed spreading area and membrane energy minimization points at a very defined state (*e.g.* distribution of intracellular components and thereby volume, size and shape) of the spread platelet. In the physiological situation, platelets are confronted with rough surfaces and structures on the micrometer scale. In such an environment an optimal spreading area is still preserved. In medicine, this physiological situation is mimicked by structuring the surface of the implant material.

Acknowledgements

The authors thank Alexander Strate, Tobias Legler and Joachim Riggert for providing platelet concentrates and for many fruitful

discussions. We acknowledge the help of Hansjörg Schwertz and Valeria Piazza for help with experimental protocols. Clean room maintenance and advice on photolithography were offered by Joachim Herbst and by Jörg Malindretos. We thank Reiner Kree for fruitful discussions. Funding was provided by the Deutsche Forschungs Gemeinschaft in the framework of the SFB 937/A12 and the Excellence Initiative.

References

1 J. G. White, in *Platelets*, ed. A. D. Michelson, Academic Press, Elsevier Science, USA, 2nd edn, 2006, ch. 3, pp. 45–73.
2 S. Schwarz, G. Henriques, R. Sandmann, A. Strate and S. Köster, *J. Cell Sci.*, 2012, **125**, 3914–3920.
3 D. B. Brewer, *Br. J. Haematol.*, 2006, **133**, 251–258.
4 M. L. Holbrook, *Proceedings of the American Microscopical Society*, 1895, **16**, 181–190.
5 W. W. Duke, *J. Am. Med. Assoc.*, 1910, **55**, 1185–1192.
6 A. Bernard, J. P. Renault, B. Michel, H. R. Bosshard and E. Delamarche, *Adv. Mater.*, 2000, **12**, 1067–1070.
7 J. L. Wilbur, E. Kim, Y. Xia and G. M. Whitesides, *Adv. Mater.*, 1995, **7**, 649–652.
8 D. C. Duffy, J. C. McDonald, O. J. A. Schueller and G. M. Whitesides, *Anal. Chem.*, 1998, **70**, 4974–4984.
9 Y. Xia and G. M. Whitesides, *Angew. Chem., Int. Ed.*, 1998, **37**, 550–575.
10 M. J. Dalby, N. Gadegaard, M. O. Riehle, C. D. Wilkinson and A. S. Curtis, *Int. J. Biochem. Cell Biol.*, 2004, **36**, 2005–2015.
11 C. J. Bettinger, R. Langer and J. T. Borenstein, *Angew. Chem., Int. Ed.*, 2009, **48**, 5406–5415.
12 P. Clark, P. Connolly, A. S. G. Curtis, J. A. T. Dow and C. D. W. Wilkinson, *Development*, 1987, **99**, 439–448.
13 R. G. Flemming, C. J. Murphy, G. A. Abrams, S. L. Goodman and P. F. Nealey, *Biomaterials*, 1999, **20**, 573–588.
14 C. C. Berry, G. Campbell, A. Spadiccino, M. Robertson and A. S. Curtis, *Biomaterials*, 2004, **25**, 5781–5788.
15 A. K. Salem, R. Stevens, R. G. Pearson, M. C. Davies, S. J. B. Tendler, C. J. Roberts, P. M. Williams and K. M. Shakesheff, *J. Biomed. Mater. Res.*, 2002, **61**, 212–217.
16 J. Y. Lim and H. J. Donahue, *Tissue Eng.*, 2007, **13**, 1879–1891.
17 L. Kikuchi, J. Y. Park, C. Victor and J. E. Davies, *Biomaterials*, 2005, **26**, 5285–5295.
18 C. Minelli, A. Kikuta, N. Tsud, M. D. Ball and A. Yamamoto, *J. Nanobiotechnol.*, 2008, **6**, 3.
19 A. Ruf and E. Morgenstern, *Semin. Thromb. Hemostasis*, 1995, **21**, 119–122.
20 J. Y. Park, C. H. Gemmell and J. E. Davies, *Biomaterials*, 2001, **22**, 2671–2682.
21 M. Zhou, J. Yang, X. Ye, A. Zheng, G. Li, P. Yang, Y. Zhu and L. Cai, *J. Nano Res.*, 2008, **2**, 129–136.
22 H. Chen, W. Song, F. Zhou, Z. Wu, H. Huang, J. Zhang, Q. Lin and B. Yang, *Colloids Surf., B*, 2009, **71**, 275–281.
23 A. Kita, Y. Sakurai, D. R. Myers, R. Rounsevell, J. N. Huang, T. J. Seok, K. Yu, M. C. Wu, D. A. Fletcher and W. A. Lam, *PLoS One*, 2011, **6**, e26437.
24 Y. Okamura, R. Schmidt, I. Raschke, M. Hintze, S. Takeoka, A. Egner and T. Lang, *Biophys. J.*, 2011, **100**, 1855–1863.
25 P. S. Sit and R. E. Marchant, *Thromb. Haemostasis*, 1999, **82**, 1053–1060.
26 X. M. Liang, S. J. Han, J. A. Reems, D. Gao and N. J. Sniadecki, *Lab Chip*, 2010, **10**, 991–998.
27 C. A. Schneider, W. S. Rasband and K. W. Eliceiri, *Nat. Methods*, 2012, **9**, 671–675.
28 A. Zemel, F. Rehfeldt, A. E. X. Brown, D. E. Discher and S. A. Safran, *Nat. Phys.*, 2010, **6**, 468–473.
29 B. Savage, S. J. Shattil and Z. M. Ruggeri, *J. Biol. Chem.*, 1992, **267**, 11300–11306.
30 D. Lehnert, B. Wehrle-Haller, C. David, U. Weiland, C. Ballestrem, B. A. Imhof and M. Bastmeyer, *J. Cell Sci.*, 2004, **117**, 41–52.
31 M. B. Villarino, *Journal of Inequalities in Pure and Applied Mathematics*, 2006, **7**, 21.